

Cold Plasma Treatment: Surface or Bulk Modification of Polymer Films?

F. Poncin-Epaillard,* J. C. Brosse, and T. Falher

Unité Mixte de Recherche Chimie et Physique des Matériaux Polymères (UMR CNRS 6515), Université du Maine, Avenue O. Messiaen, 72000 Le Mans, France

Received October 24, 1996; Revised Manuscript Received April 15, 1997[®]

ABSTRACT: Reactive species of nitrogen cold plasma could interact with a polymeric surface, leading to an important surface functionalization (mostly as amino group attachment) and consequently to a surface having a Lewis base character. Under certain conditions, the surface functionalization is not the only modification; a morphologic transformation is also noticed. The virgin isotactic polypropylene is composed in bulk of smectic and amorphous phases in the same proportions, and after the plasma treatment a more organized monoclinic α phase appears. During the plasma treatment, two types of crystallization take place, smectic phase \rightarrow α phase and also amorphous \rightarrow smectic phase, their respective proportions varying in the thickness of the film. This phenomenon could be explained by an absorption of the plasma VUV radiations by the polymer film. Illustration is given with different plasmas for which the VUV emission is important.

Introduction

The opportunity of compounding polymeric materials has emphasized their application and use in various industrial fields. However, the need, incessantly increasing, of macromolecular materials with specific characteristics commands, rather than new material elaboration, properties improvement, in particular the surface properties in fields such as painting, adhesion, etc. At the moment, the major goal of the research in such fields is focused on surface study and on the possibility of a control of surface properties depending on the industrial use.

To achieve such material with controlled surface properties, several techniques were applied, such as chemical oxidation, flame and mechanical radiations, and plasma treatments.¹ If, in most cases, the surface modification is well described in terms of physicochemical and chemical characterizations, little attention is focused on the morphologic properties either on the surface or in the film thickness. Do these different treatments affect the bulk?

Plasma etching of polymers was studied in relation to the surface polymer crystallinity.^{2,3} Ablation with air plasma occurs mainly in the amorphous region of polypropylene and with prolonged treatment the polymer surface becomes rough enough to have a microdomain structure.³ Polymers like poly(ether-urethane)s that contain hard and soft segments show a surface mostly composed of hard segments (urethane) when submitted to a plasma etching, and these modifications seem to be temporary over a period of 6 months.³ Fluorination of different crystalline polymers (Nylon 6 and PET) was investigated, and for the authors, the plasma did not change the film crystallinity.⁴

Here, illustrations of morphologic transformations are given for the cold nitrogen plasma treatment of isotactic polypropylene. The surface modification of polypropylene has been characterized in previous publications.^{5–8}

Experimental Part

Materials. Polypropylene. Exempt of any kind of additives, polypropylene, supplied by Institut Textile de France (ITF) and

obtained by extrusion, was synthesized with Ziegler-Natta catalyst in a heterogeneous phase. It is an isotactic semicrystalline polymer (melting point: 160 °C). The crystalline phase corresponds to a smectic state in a proportion of 52–55% (determined respectively by X-ray scattering and IR spectroscopy) and 62% (determined with differential scanning calorimetry).

Purity of gases, purchased from Air Liquide, is as follows: nitrogen (grade U), purity >99.998%; oxygen (grade C), purity $\geq 99.5\%$; hydrogen (grade C), purity >99.995%; helium (grade C), purity >99.995%.

Plasma Equipment and Plasma Treatment. The equipment used here is a microwave plasma apparatus composed of three parts. The excitation is provided by a microwave generator (433 MHz) with a variable power (0–250 W), which is coupled to a resonant cavity. The incident power (P_i) and the reflected power (P_r) are measured with a power meter (Hewlett-Packard, 435B). The impedance is adjusted until the reflected power is very low ($P_r < 10^{-2}$ W). The glow is generated at the top of the reactor. The pumping system is composed of a primary pump (CIT Alcatel 2012) and an oil diffusion pump (CIT Alcatel Crystal). The gas flow (D) is controlled by a MKS mass flowmeter type 1259B. The pressure (p) is measured with Penning and Pirani gauges. The reactor is a quartz cylinder of 500 mm length and 76 mm diameter. The reactor is set up on a chamber used for the sample introduction. The substrate can be moved in or out of the plasma volume. We note d , the distance between the bottom of the excitator and the sample, and l , the plasma length.

Before each run, the system was kept at 10^{-6} mbar for at least 2 h. The plasma treatment procedure was as follows: after the film was set up on the substrate, the reactor pressure was reduced below 2×10^{-5} mbar and the gas was introduced 5 min before the treatment. Then the latter is achieved. Two conditions were chosen: A, $P_i = 60$ W, $t = 2$ min, $D = 20$ sccm, $p = 0.3$ mbar, $d = 10$ cm, $l = 15$ cm; B, $P_i = 100$ W, $t = 5$ min, $D = 20$ sccm, $p = 0.3$ mbar, $d = 4$ cm, $l = 20$ cm.

These conditions correspond to two types of surfaces:⁸ the former leads to a surface highly functionalized but with a low surface radical concentration; the latter gives a surface with a low amino group concentration and a high radical density.

Spectroscopy of Optical Emission. Emission spectroscopy was performed with a Jobin Yvon HR 320 monochromator with a focal length of 32 cm equipped with two 1200 grooves/mm gratings, and the photons were detected with a Hamamatsu R928 photomultiplier whose spectral response ranges from 185 to 950 nm. The spectrometer resolution was 0.1 nm, and the output signal acquired through an optical fiber was amplified by a spectralinke (Jobin Yvon) controlled by a

[®] Abstract published in *Advance ACS Abstracts*, July 1, 1997.

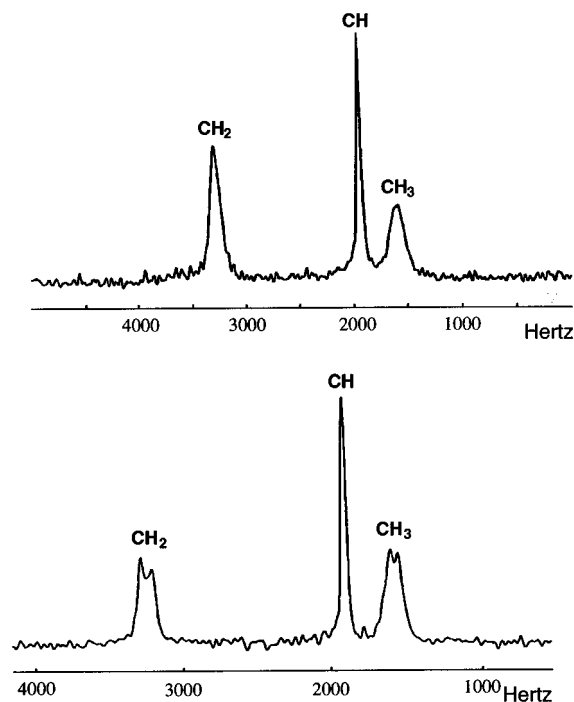


Figure 1. ^{13}C NMR spectra of polypropylene blank, treated under conditions a (top) or b (bottom).

computer. The sample position was maintained on the axis of the optical probe.

Solid State Nuclear Magnetic Resonance (NMR). The analyses were run on a BRUKER MSL 300 MHz spectrometer at the Laboratoire de Physique de l'Etat Condensé (URA 807) of Université du Maine.

X-ray Scattering. The X-ray scattering apparatus, a prototype built in the Laboratoire de Physique de l'Etat Condensé (URA 807) of Université du Maine, is composed of 4 parts: the XR beam (generator PHILLIPS PW 1130/00/60, copper anticathod), the goniometer (two circles HUBER 424 set down onto two superposed X, Y translation tables, a plane monochromator, plus several vertical slots to focus the beam), the detector (BICRON type) with an electronic system (Inel type), and the controller system (model INEL XRGCI) to control the shift of the sample and the detector. All the analyses are run in transmission mode.

FTIR Spectroscopy. The FTIR analyses run on a spectrometer (Perkin-Elmer no. 1750) were made in transmission mode (resolution, 4 cm^{-1} ; 20 scans) or in specular reflection mode at variable incidence angles ($45\text{--}60^\circ$) (resolution, 2 cm^{-1} ; 200 scans).

DCS Analyses. The analyses were run on a TA Instrument SDT 2960 apparatus at CTTM-département matériaux IRAP, Le Mans France. The thermograms were recorded from 30 to 200°C with a temperature increase of $10^\circ\text{C min}^{-1}$ under argon flux.

Results

After the surface characterization of the plasma-modified polypropylene films, described elsewhere,⁸ the crystallinity study was run on all the volume of the samples. Different analytical techniques were explored: ^{13}C solid state NMR, X-ray diffraction, transmission FTIR spectroscopy, and differential scanning calorimetry (DCS).

^{13}C solid state NMR analyses. The ^{13}C solid state NMR spectrum of virgin or treated under conditions a samples (Figure 1a) is typical of a polypropylene smectic phase.^{11,13} Because of its only one interhelical distance (6.50 Å), the resonance signals assigned to the methenyl (CH), methylene (CH_2), and methyl groups (CH_3) are

singlets. Treatment under conditions b leads to another effect on the polymer film, since the NMR spectrum (Figure 1b) presents doublets for the methyl and methylene groups that can be assigned to the existence of two different interhelical distances (5.28 and 6.14 Å), which are smaller than the former one and are indicative of an α crystalline phase.¹⁴ Therefore, interactions such as van der Waals interactions favor the intermolecular chains interactions leading to the α phase organization set up.¹⁴ The methenyl peak is still represented as a singlet, since the corresponding groups bound to side methyl groups are protected against intermolecular effects.¹⁴ So nitrogen plasma under conditions b leads to a crystallization of the smectic phase into the α one. The structural modification takes place in a noticeable thickness, since NMR spectroscopy is a bulk analysis. On the other hand, solid state NMR is not sensitive enough to give evidence of functionalization characterized elsewhere.⁸

X-ray Diffraction. X-ray diffractograms (Figure 2a) of virgin and modified samples under conditions a have two major reflections at $2\theta = 15^\circ$ and 21° , both corresponding to the smectic phase.^{13,15} Their relative important width reveals a partially ordered phase. On the other hand, the more diffused third reflection at $2\theta = 17^\circ$ is relative to the amorphous phase. The X-ray diffractogram of a sample modified under conditions b (Figure 2b) shows five intense reflections plus two smaller ones assigned to the α crystallization phase of polypropylene.^{13,16} Once again, evidence is given of a bulk structural modification. However, the presence of a (100) reflection corresponding to the smectic form suggests that the crystallization process is incomplete even after 10 min of treatment. The structural change is a continuous phenomenon depending on the treatment duration (Figure 3) and results in a progressive macromolecular chain organization¹⁷ with a higher order level through intermolecular interactions. This reorganization needs lateral motions or chain turnover to form helical rows with the same configuration.¹⁵ A simulation program ("fullprof") was applied to rebuild the X-ray diffractogram while taking into account the same crystallographic parameters, such as space group ($P2_1/c$) and the carbon atom coordinates (9 atoms/period) in the 3_1 helix of isotactic polypropylene.¹⁹ The results given in Table 1 and Figure 4 show that calculated values are in good agreement with observation and the literature.^{18–22}

Transmission FTIR Spectroscopy. FTIR spectrum of polypropylene shows absorption bands corresponding to the structure regularity of isolated helices or crystalline zones at 1220 , 1168 , 998 , 900 , 841 , and 809 cm^{-1} and absorption bands corresponding to the disorder or amorphous phase at 1460 , 1256 , 1171 , and 973 cm^{-1} .^{23–25} Among these absorption bands, two of them (at 973 and 998 cm^{-1}), corresponding to the valence vibration of C–C bonds, were chosen because of their good resolution and sensitivity for short segments (respectively 4–5 and 10–11 constitutive units^{24,25}). Their absorbance ratio, avoiding any fluctuation due to the thickness variation, is given in Table 2 for the three samples. The absorbance ratio increases when the sample is treated under conditions b, leading to the concept of an order development in the matrix, as also shown in NMR and X-ray analysis. No variation is noticed for sample treated under conditions a.

DSC Measurements. The thermogram of a sample modified under conditions a, similar to the blank one

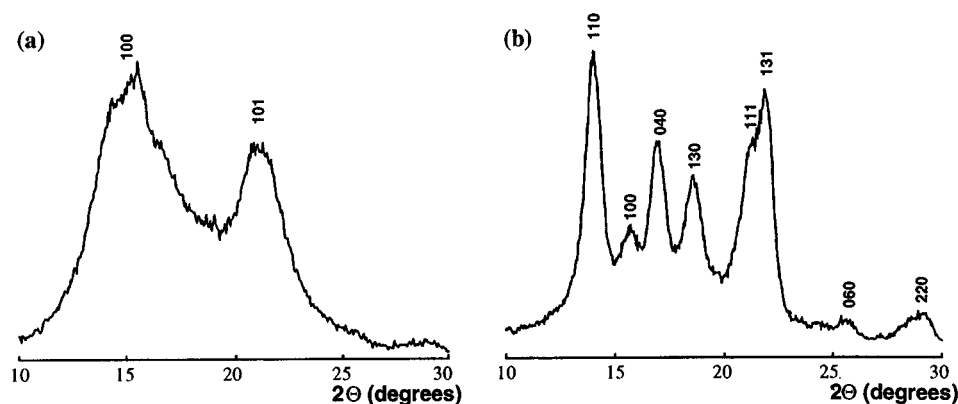


Figure 2. X-ray diffractograms of polypropylene blank, treated under conditions a or b.

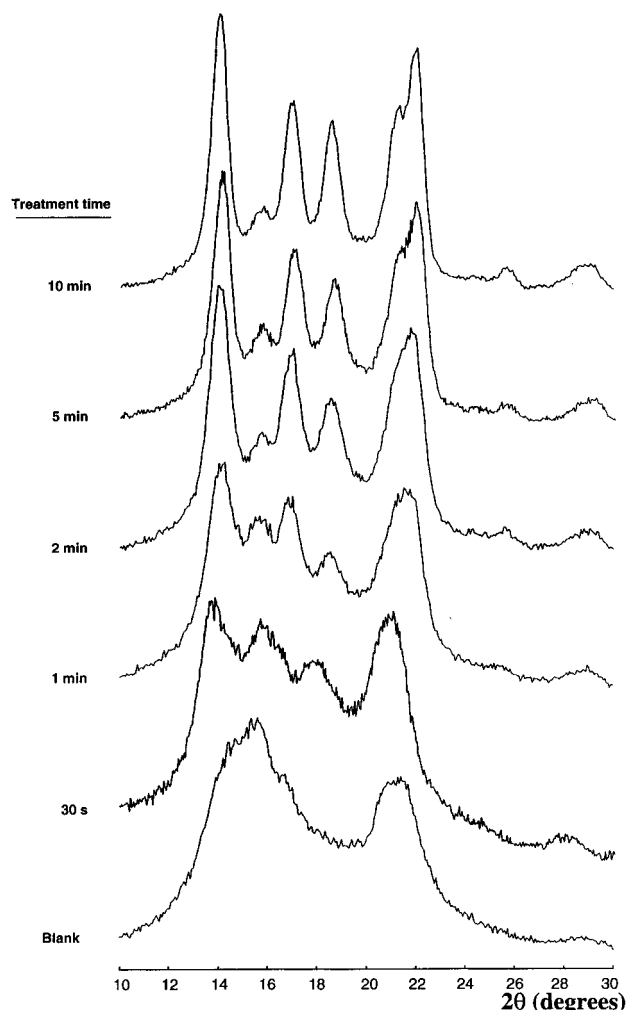


Figure 3. Dependence versus treatment time of structural phase of polypropylene modified under conditions b, followed by X-ray diffraction.

(Figure 5), shows only an endothermal peak (maximum at 70 °C) related to the α crystallization induced by the polymer heating during the analysis. Plasma exposition under such conditions does not affect the polymer morphology. After the treatment under conditions b (Figure 5), the peak corresponding to the α phase transition does not remain on the thermal diagram due to the crystallization of an important fraction of the smectic phase into the α phase during plasma treatment. Moreover, a shoulder appears for temperatures between 135 and 150 °C which could be assigned to the

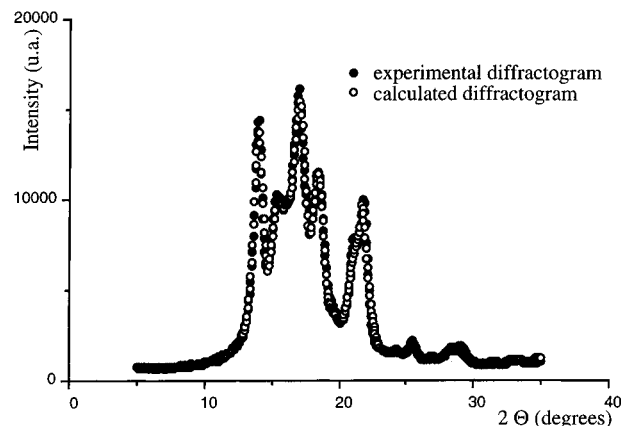


Figure 4. X-ray diffractogram simulation of structural organization of polypropylene modified under conditions b.

Table 1. Position and Intensity of the Different Rays Observed (I_o) and Calculated (I_c) for the α Crystalline Phase for Sample Treated under Conditions b

hkl	2θ (deg)	I_o	I_c
110	14.12	4077	3926
040	17.22	3378	3441
130	18.67	4003	4228
111	21.24	1366	1496
131	21.98	2009	2114
041	22.13	133	131
150	25.50	161	165
060	25.70	389	414
220	28.45	282	282

Table 2. Dependence versus Duration of Absorbances A_{998}/A_{973} Ratio of Polypropylene Blank, Treated under Conditions a or b

	virgin sample	sample treated under conditions a	sample treated under conditions b
A_{998}/A_{973}	0.80	0.82	0.95

recrystallization of the α phase form into another α phase form more stable and having a higher order level.²⁶ This transformation corresponds to the partial melting of the primitive spherulites and leads to an increase in melting enthalpy²⁶ (Table 3).

Crystallinity Yield Determination. From the different X-ray diffractograms, evidences are given on the presence of three morphologic phases, i.e. α , smetic, and amorphous phases. The crystallinity yield is proportional to the ratio of two areas on the X-ray diffractogram, the first one (A_o) corresponding to the narrow peaks characteristic of the α crystalline morphology and the second one assigned to the continuum background of the amorphous and smectic structure diffraction

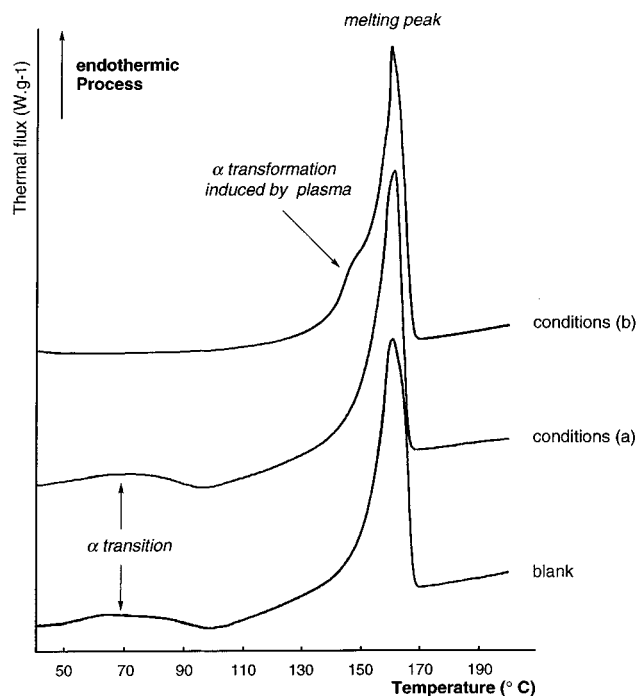


Figure 5. DCS thermograms of polypropylene blank, treated under conditions a or b.

Table 3. Melting Point and Enthalpy of Polypropylene Virgin Treated under Conditions a or b

	virgin sample	sample treated under conditions a	sample treated under conditions b
T_m (°C)	161.1	164.2	160.9
ΔH (J g ⁻¹)	90.5	91.2	97.7

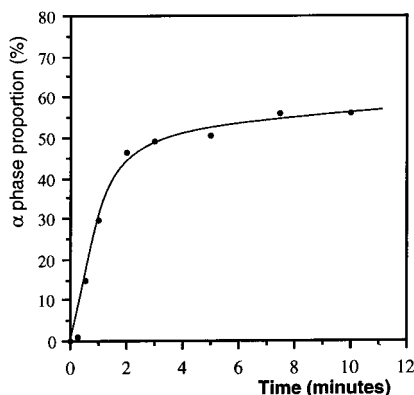


Figure 6. Dependence of α crystalline phase proportion versus treatment time for sample treated under conditions b (X-ray scattering calculation).

($A_{(am+sm)}$), where all X-rays are diffused in any direction.^{16,27,28}

$$\% \alpha = \frac{A_{\alpha}}{A_{\alpha} + A_{(am+sm)}}$$

The α phase proportion increases quickly during the first 2 min of treatment and then increases slowly to reach a plateau at 55% (Figure 6), a value corresponding to the virgin sample one (smectic proportion calculated from X-ray analysis, 52%). For long treatments (duration longer than 10 min), the (100) reflection corresponding to the smectic phase is still remaining on the X-ray diffractogram. So these two facts may lead us to concede to the possibility of another rearrangement corresponding to the change of amorphous into smectic phase.²⁹

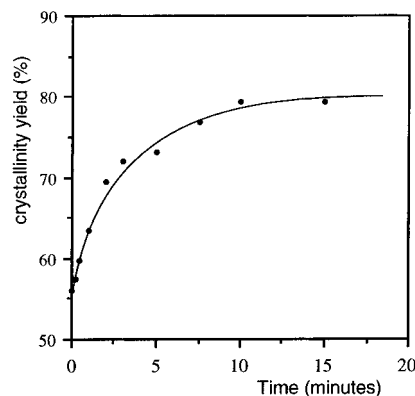


Figure 7. Dependence of the all crystalline phase proportion versus treatment time for sample treated under conditions b (FTIR spectroscopy calculation).

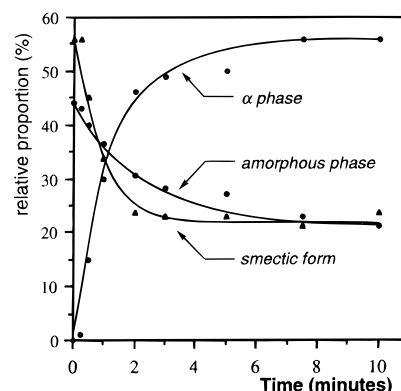


Figure 8. Dependence of the different structural phase proportions versus treatment time for sample treated under conditions b.

The crystallinity rate (C_r) is also proportional to the film density:³⁰

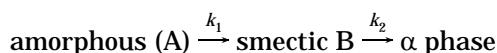
$$\% Cr = \frac{d - d_{am}}{d_{cr} - d_{am}}$$

with d_{am} , the density of the amorphous polypropylene (0.853 at 25 °C) and d_{cr} the density of the crystalline material (0.935 at 25 °C). On the other hand, the absorbance peak ratio (A_{998}/A_{973}) in the FTIR spectrum is related to the polypropylene density³⁰ as follows:

$$A_{998}/A_{973} = -9.49 + 11.43d$$

So the crystallinity yield, determined through FTIR spectroscopy as described before, is increasing versus plasma duration (Figure 7) until reaching a plateau at 78% for 10 min of treatment. Here, the second type of crystallization (amorphous \rightarrow smetic) is confirmed.

From the two calculations of the crystallization yield and the α phase proportion, the smectic phase concentration was deduced. Their respective dependences versus treatment time illustrated in Figure 8 show that, in parallel with the α phase crystallization, the smectic and amorphous phases disappear, reinforcing the idea of two types of crystallization.¹⁰ The smectic \rightarrow α phase rearrangement takes place during the first 3 min of the plasma treatment, and the other transformation, i.e. crystallization of the amorphous phase into the smectic phase, is more slow and moderate. A kinetic study, corresponding to two successive step reactions between three compounds



was run, and the two rate constants k_1 and k_2 were determined as well as the half-life time (Table 4). The low value of $t_{1/2}$ indicates fast crystallization processes.

Discussion

The crystallizations need energy input that could be provided from an undirect thermal effect or from very energetic species such as VUV radiations, which can affect a film thickness higher than 10 μm .

For an evaluation of the thermal effect, an approach of the gas temperature is given with the determination of the rotational temperature of molecular nitrogen in the $\text{C}^3\Pi_u$ radiative state.^{32–33} For the two chosen conditions (a and b), the rotational temperature is respectively found around 180 and 275 °C. These quite high values suggest an overestimated measurement in comparison with the real gas temperature. Indeed, a plasma temperature higher than the polymer melting point (162 °C determined with DSC) should lead to its strong degradation. However, little or no degradation is noticed under both plasma conditions.⁸ The overcalculation could be provided by a not so good resolution of the triplet rotational band and an error in the measurement. If the thermal effect exists, it is higher under conditions b. To avoid any undirect thermal effect, some experiments were run with a sample cooling system (the freezing liquid was liquid nitrogen) in another RF plasma reactor with close conditions of pressure, power, and duration. A crystallization still exists but not in such a high proportion. So the thermal effect affects the material but is not the predominant one.

The emission of radiations with short wavelengths, more and more mentioned in the literature,^{34–37} as an important agent of polymer chemical modification depends strongly on gas nature, in the order H_2 plasma > N_2 plasma > O_2 plasma > He plasma.³⁷ Different polypropylene films were treated in H_2 , N_2 , O_2 , and He plasmas under conditions b. The gas nature directly influences the α crystallization kinetics, described in Figure 9. O_2 plasma is the most efficient, and helium is the last efficient one in terms of structural modification. From the spectra measured by Hollander and co-workers,³⁷ a mean intensity of the VUV emission peaks in the different microwave plasmas is determined, and the dependence of α phase fraction versus the mean emission intensity was reported in Figure 10. For the treatments in He, N_2 , and H_2 plasmas, the radiative flux and the structural modification of polypropylene are exponentially dependent. Therefore, the VUV radiations could be a major agent of the structural change in such a bulkiness, depending on the energy level, as defined in the Beer–Lambert law. On the contrary, the oxygen plasma leads to a higher α phase proportion than what could be deduced from its VUV emission, and that could be explained through the attachment of oxidized groups during the plasma treatment. The new surface functions are, in most cases, chromophore groups, and therefore they could emphasize the sensitivity of the polymer film toward the radiations.

The depth of structural modification shown in Figure 11 depends on the chemical nature of the plasma gas. The crystallinity composition of the virgin sample is not uniform; the superficial crystallinity is more important (78%) than the bulk one (56%). For the treated sample, there is a linear relationship between the structural

Table 4. Determination of Kinetic Parameter of Polypropylene Modified under Conditions b

	amorphous phase ^a	α phase ^a	smectic phase ^b
kinetic law	$\frac{d[A]}{dt} = -k_1[A]$	$\frac{d[C]}{dt} = -k_2[B]$	$\frac{d[B]}{dt} = -k_1[A] - k_2[C]$
k (min^{-1})	0.42	0.90	1.30
$t_{1/2}$ (min)	1.65	0.77	0.53

^a Determined from Figure 8. ^b Theoretical value of an apparent k obtained by mathematical simulation.

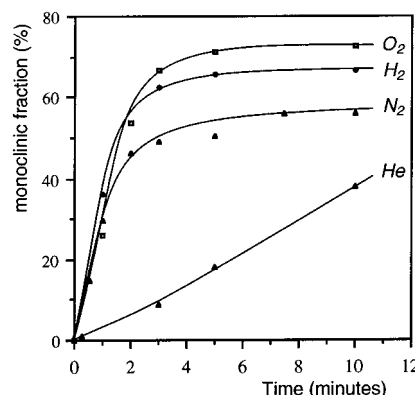


Figure 9. Dependence of α crystalline phase proportion versus treatment time and plasma chemical nature for sample treated under conditions b (X-ray scattering calculation).

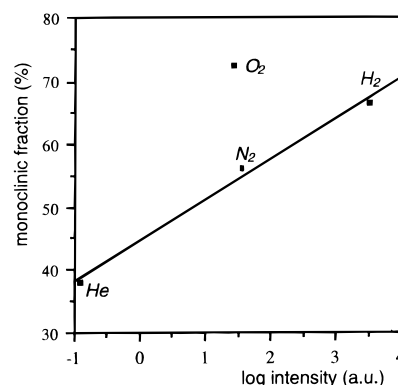


Figure 10. Relationship between the α crystalline phase proportion appearance and the various plasma VUV emissions for sample treated under conditions b (X-ray scattering calculation).

state of the film and the analyzed thickness, and a similar reactivity order for the decrease of the crystalline fraction versus film thickness is found whatever the plasma chemical nature.

The absorption of photons at wavelengths lower than 160 nm leads to the electronic excitation $\sigma \rightarrow \sigma^*$ of C–C and C–H bonds.³⁸ Depending on the proportion of energy absorbed by the polymer, two effects can take place: (i) homolytic scission³⁹ of bonds corresponding to macroradical formation followed by degradation, cross-linking, and functionalization reactions and (ii) thermal transfer of the excess energy through vibrational relaxation and local molecular motions.^{40–42}

A polymeric film absorbs a certain proportion of radiative energy that decreases in the volume depending on the concentration of photosensitive groups or molecules such as C–C and C–H bonds. The C–C and C–H bond scissions, needing an excess of energy respectively of 3.61 and 4.30 eV, could be only a superficial phenomenon, as shown elsewhere.⁸ On the

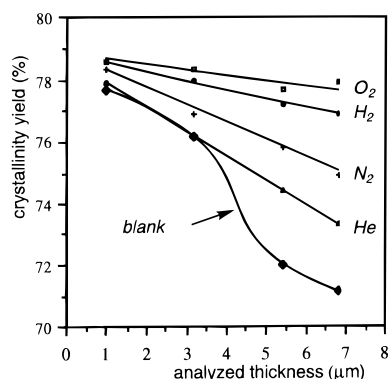


Figure 11. Gradient of the α crystalline phase proportion with the thickness of polypropylene treated in various plasmas under conditions b (X-ray scattering calculation).

other hand, the thermal relaxation phenomenon resulting from a lower energetic transfer could lead to local chain rearrangements, behind a threshold thickness where the absorbed energy is lower than that corresponding to the atom motion, since the α transition requires a low energy level (16 J g^{-1} of polymer).¹⁰ The thermal relaxation phenomenon could explain the structural modification and the observed gradient of crystallinity in the thickness.

Conclusion

Reactive species of the nitrogen plasma induce the formation of macroradicals onto the polypropylene surface. These latter, recombined or reacted with gaseous fragments, control the cross-linking or functionalization reactions onto the surface. Besides these modifications, plasma treatment under certain conditions could favor an increase of the film crystallinity and even the appearance of a new crystallization with a concentration gradient depending on the film thickness.

A relationship between the crystallinity changes and the plasma emission characteristics, including VUV radiation, was found: a hydrogen plasma having the more important VUV emission affects more strongly the crystallinity of the polypropylene film. The energetic radiation absorptions produce thermal relaxations leading to deep local chain rearrangements as well as the structural modification involved in annealing.

References and Notes

- (1) Legeay, G.; Brosse, J. C.; Epaillard, F. *Double Liaison—Chim. Peint.* **1986**, 367–368, 111.
- (2) Ogita, T.; Ponomarev, A. N.; Nishimoto, S.; Kagiya, T. *J. Macromol. Sci. Chem.* **1985**, A22 (8), 1135.
- (3) Vargo, T. G.; Hook, D. G.; Gardella, J.; Eberhardt, M. A.; Meyer, A. E.; Baier, R. E. *J. Polym. Sci., Polym. Chem. Ed.*, **1991**, 29, 535.
- (4) Yasuda, T.; Okuno, T.; Yoshida, K.; Yasuda, H. *J. Polym. Sci., Polym. Phys. Ed.* **1988**, 26, 1781.
- (5) Poncin-Epaillard, F.; Chevet, B.; Brosse, J. C. *J. Adhesion Sci. Technol.* **1994**, 8 (4), 455.
- (6) Poncin-Epaillard, F.; Chevet, B.; Brosse, J. C. *Makromol. Chem.* **1991**, 192, 1589.
- (7) Chevet, B. Réaction de post-greffage sur des polymères activés par un plasma froid ou un faisceau d'électrons. Thèse de l'Université du Maine, 1992.
- (8) Falher, T. Post-greffage de la N-vinyl-2-pyrrolidone sur un film de polypropylène modifié par plasma froid d'azote. Thèse de l'Université du Maine, 1996.
- (9) Natta, G. *Makromol. Chem.* **1960**, 35, 93.
- (10) Gailey, J. A.; Ralston, R. H. *SPE Trans.* **1964**, 4, 29.
- (11) Bunn, A.; Cudby, M. E. A.; Harris, R. K.; Packer, K. J.; Say, B. J. *Polymer* **1982**, 23, 694.
- (12) Border, G.; Grell, M.; Kallo, A. *Faserforsch. Textil-Tech.* **1964**, 15, 527.
- (13) Tanaka, H. *Eur. Polym. J.* **1991**, 27 (7), 565.
- (14) Lotz, B. *Macromol. Chem. Symp.* **1995**, 94, 97.
- (15) Mc Allister, P. B.; Carter, T. J.; Hinde, R. M. *J. Polym. Sci., Polym. Phys. Ed.* **1978**, 16, 49.
- (16) Miller, R. L. *Polymer* **1960**, 1, 135.
- (17) Zannetti, R.; Celotti, G.; Fichera, A.; Francesconi, R. *Makromol. Chem.* **1969**, 128, 137.
- (18) Mencik, Z. *J. Macromol. Sci.* **1972**, B6 (1), 101.
- (19) Ferro, D. R.; Brückner, S.; Meille, S. V.; Ragazzi, M. *Macromolecules* **1992**, 25 (20), 5231.
- (20) Turner-Jones, A.; Aizlewood, J. M.; Becket, D. R. *Macromol. Chem.*, **1964**, 75, 134.
- (21) Stocker, W.; Magonov, S. N.; Cantow, H. J.; Wittmann, J. C.; Lotz, B. *Macromolecules*, **1993**, 26 (22), 5915.
- (22) Nishimoto, S.; Kagiya, T. In *Handbook of Polymer Degradation*; Hamid, S. H.; Amin, M. B.; Maadhad, A. G., Eds.; Marcel Dekker Inc.: New York, 1992; p 3.
- (23) Glotin, M.; Rahalkar, R. R.; Hendra, P. J.; Cudby, M. E. A.; Willis, H. A. *Polymer* **1981**, 22, 731.
- (24) Burfield, D. R.; Loi, P. S. T. *J. Appl. Polym. Sci.* **1988**, 36, 279.
- (25) Kissin, Y. V.; Rishina, L. A. *Eur. Polym. J.* **1976**, 12, 757.
- (26) Awaya, H. *Polymer*, **1988**, 29, 591.
- (27) Weidinger, A.; Hermans, P. H. *Makromol. Chem.*, **1961**, 50, 98.
- (28) Wyckoff, H. W. *J. Polym. Sci.*, **1962**, 62, 83.
- (29) Hendra, P. J.; Vile, J.; Willis, H. A.; Zichy, V.; Cudby, M. E. A. *Polymer*, **1984**, 25, 785.
- (30) Hobbs, J. P.; Sung, C. S. P.; Krishnan, K.; Hill, S. *Macromolecules*, **1983**, 16 (2), 193.
- (31) Quynn, R. G.; Riley, J. L.; Young, D. A.; Noether, H. D. *J. Appl. Polym. Sci.* **1959**, 2 (5), 166.
- (32) Ricard, A. *Plasmas Réactifs*; Société Française du Vide: Paris, 1995; p 87.
- (33) Schadee, A. *Bull. Astron. Inst. Neth.* **1964**, 17, 311.
- (34) Takacs, G. A.; Vukanovic, V.; Chen, J. X.; Egitto, F. D.; Matienzo, L. J.; Emmi, F. *Polym. Degrad. Stab.* **1993**, 40, 73.
- (35) Yasuda, H. *J. Macromol. Sci. Chem.* **1976**, A10, 383.
- (36) Shard, A. G.; Badyal, J. P. S. *Polym. Commun.* **1991**, 32, 217.
- (37) Holländer, A.; Klemberg-Sapieha, J. E.; Wertheimer, M. R. *J. Polym. Sci., Polym. Chem. Ed.*, **1995**, 33, 2013.
- (38) George, R. A.; Martin, D. A.; Wilson, E. G. *J. Phys. C, Solid State Phys.* **1972**, 5, 871.
- (39) Perrin, J.; Schmitt, J. *Réactivité dans les plasmas*; Ecole d'été; Aussois (France) août, 1983; Les Editions de Physique, Paris, 1984; p 91.
- (40) Carter, G.; Nobes, M. J.; Katardjiev, I. V. *Vacuum*, **1988**, 38 (6), 479.
- (41) Yabe, A.; Niimo, H. *Mol. Cryst. Liq. Cryst.* **1993**, 224, 111.
- (42) Minkova, L.; Lefterova, E.; Koleva, T.; Nedkov, E.; Nikolova, M. *Colloid Polym. Sci.* **1988**, 266, 298.

MA961585D